JTTEES 2:121-126

Measurement of Imperfections in Thermal Spray Coatings Using Synchrotron-Computed Microtomography*

P. Spanne, K.W. Jones, H. Herman, and W.L. Riggs

The determination of microstructural imperfections in thermal spray coatings using nondestructive synchrotron-computed microtomography (CMT) is described. This technique provides spatial resolutions in the 2- to 4-μm range, enabling identification of cracks and voids. Comparisons with other conventional methods for identifying microstructural features in coatings are made.

1. Introduction

THE central question within the thermal spray coating community is the matter of imperfections within the sprayed deposit and the ways in which these imperfections influence properties. This article addresses the topic of "macroscopic" imperfections, which are greater than 1 μm in dimension. These imperfections include cracks and voids that originate from less than optimum processing conditions and, in some cases, post-processing thermal cycling (e.g., thermal barrier coatings, or TBCs). Sometimes, improperly sized feedstock particles lead to the incorporation of unmelted particles, which can yield cracks and voids. In some cases, the voids are describable as through-porosity, thus enabling for example ingress of corrodents with subsequent attack of interfaces leading to delamination. It is thus essential to be able to detect and to characterize imperfections.

Traditionally, optical metallography has been used to detect and describe cracks and porosity. However, a serious problem with metallographic techniques is the need to mount, section, and polish the coated part. Difficulties arise in this procedure, including pulling-out of splats and unmelted particles, which under metallographic examination commonly appear as voids. In the case of the softer metals, smearing during polishing is a problem, which in effect closes the porosity. In both cases, an incorrect assessment of porosity content and its geometry may be made.

The general problems associated with traditional metallographic methods are presented in Ref 1. Of special relevance to the present work is a recent metallographic characterization program at GE in Cincinnati,[2,3] in which the effectiveness of metallographic analysis using traditional mounting and polishing techniques was assessed. For example, if particles of the coating are being removed by polishing (pullouts), how can these apparent voids be unambiguously differentiated from actual process-related pores? One answer to this question is to use synchrotron-computed microtomography (CMT) for nondestructive examination of these materials, thus avoiding sample preparation artifacts. It is thus possible to characterize cracks and voids without disturbing their features and even to provide a three-dimensional view of a coating.

A brief overview of CMT is given below. To illustrate the capability of the CMT technique in microcharacterization of thermal spray coatings, computed tomograms from two specimens are presented and compared, with the expected results based on the quality of the feedstock powder and the spray process parameters.

Keywords: imperfections, microtomography, porosity, synchrotron-computed microtomography, thermal barrier coatings, computed tomography

P. Spanne and **K.W. Jones,** Brookhaven National Laboratory, Upton, New York; **H. Herman,** State University of New York, Stony Brook, New York; and **W.L. Riggs,** GE Aircraft Engines, Cincinnati, Ohio.

*Work supported by the US Department of Energy under Contract No. DE-AC02-76CH00016.

2. Experimental Method

2.1 *Synchrotron-Computed Microtomography*

Computed microtomography is a method well suited to microscopic nondestructive evaluation (NDE) of materials. The risk of sample preparation-induced artifacts is minimized because no physical sectioning of the sample is required. The spatial resolution, which can be attained using conventional x-ray tubes, is limited mainly by the source spectral brightness and is generally much greater than 20 μm. The recent introduction of electron storage rings dedicated to synchrotron x-ray production has made available x-ray sources with 3 to 4 orders of magnitude higher brightness. A comparison of the brightness of a conventional x-ray tube and several synchrotron x-ray sources are shown in Fig. 1. The range in brightness of x-ray tubes is shown as the shaded region in the lower part of the diagram, and the acronyms for the synchrotron sources are National Synchrotron Light Source (NSLS), Stanford Synchrotron Radiation Laboratory (SSRL), Advanced Light Source (ALS), Positron-Electron-Project (PEP), and European Synchrotron Radiation Facility (ESRF). The high synchrotron brightness permits CMT measurements with spatial resolutions down to 2 to 4 μm (see, for example, Ref 4 to 6). Synchrotron x-ray CMT therefore presents a unique method for microscopic NDE of thermal spray coatings.

The measurements reported here were made using a bending magnet x-ray source at the National Synchrotron Light Source

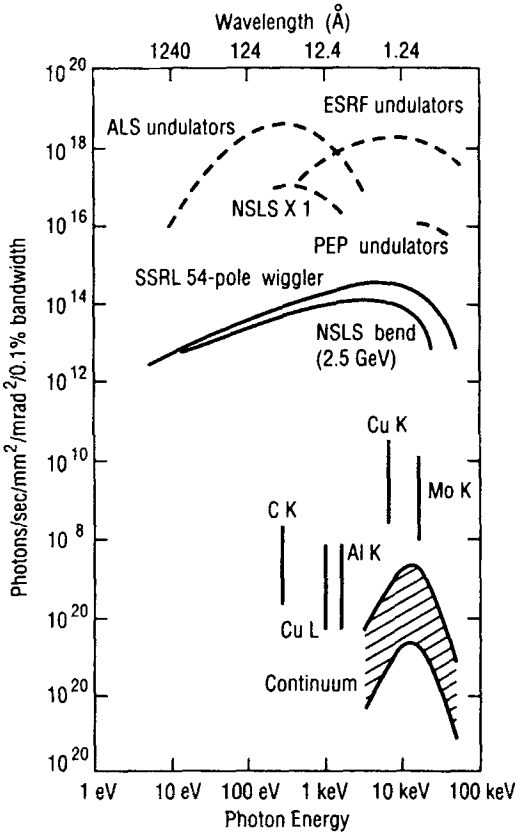

Fig. 1 Spectral brightness for several synchrotron radiation sources and conventional x-ray sources. The data from conventional x-ray tubes should be taken as rough estimates only, because brightness depends strongly on such parameters as operating voltage and take-off angle. The indicated two order of magnitude ranges show the approximate variation that can be expected among stationary anode tubes (lower end of range), rotating anode tubes (middle), and rotating anode tubes with microfocusing (upper end of range) (Ref 7).

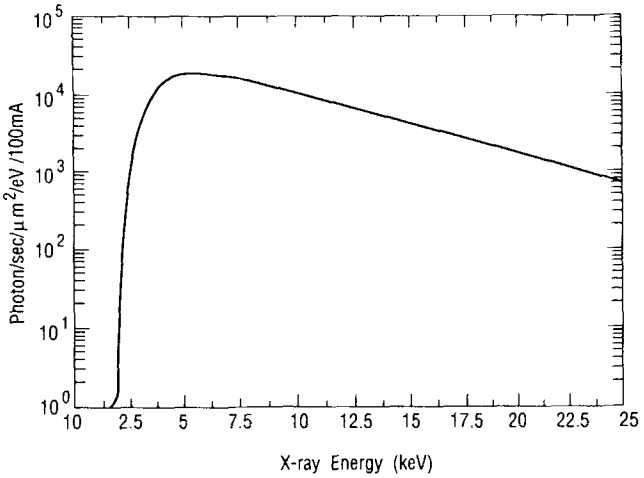

Fig. 2 Energy spectrum of x-rays from NSLS bending magnet source. Photon fluence rate per 100 mA ring current 10 m from the electron orbit.

Table 1 Coatings examined using CMT

Coating No.	Description
A98	Tungsten carbide/cobalt; externally injected powder (Metco 7M) onto steel substrate; fairly porous
B99	Tungsten carbide/cobalt; internally injected powder (Plasmadyne SG-100) onto steel substrate; much more dense than A98

at Brookhaven National Laboratory (BNL). Figure 2 shows the continuous energy spectrum from this source. The low-energy cutoff results from attenuation of x-rays in the beryllium windows that separate the CMT apparatus from the ultrahigh vacuum in the electron storage ring. The x-ray energy spectrum was modified by metal filters to match the sample composition and size.[4] For the measurements on the tungsten carbide/cobalt thermal spray specimens, a 250-μm thick hafnium filter was used.

A first-generation CMT scanner, operated in x-ray absorption mode, was used to study the morphology of thermal spray specimens.[4] First-generation CMT devices use a rotate-translate sample movement scheme through a pencil beam of synchrotron x-rays during data collection. The relative transmission of the incident x-rays is measured for each radial and azimuthal point. The resulting data sets were used to reconstruct tomograms representing maps of the x-ray absorption properties in the samples. The quantity represented by the pixel values is an average of the linear attenuation coefficient over the energy spectrum of the x-rays and the materials in the volume resolution element. Data collection was made with pencil beams having areas down to 3×4 μm^2. The resulting tomograms therefore have pixel sizes of 3 to 4 μm, and a tomographic slice thickness of 4 μm.

The image reconstructions were performed using a filtered backprojection algorithm on a Digital Equipment Corporation MicroVAX-III computer. The reconstruction time varies with the number of pixels in the image matrix and ranged typically from a few up to 15 min. Repetition of the imaging for several contiguous planes through a sample leads to a three-dimensional representation of the x-ray absorption, as expressed by the linear attenuation coefficient, μ, within a single sample.

2.2 *Specimen Preparation*

Although measurements on specimens from a whole series of thermal sprayed coatings have been carried out, this discussion is limited to one key example—the plasma spraying of tungsten carbide/cobalt in air using both external powder injection, processed to result in relatively inefficient melting, and internal powder injection, resulting in more efficient melting (Table 1). It is anticipated that the internal powder injection, specimen B99, should result in a more homogeneous coating with less porosity than the coating achieved through external injection, specimen A98.

Small fragments of coatings were obtained from plasma spray coatings deposited on steel. They were loosened from the steel substrate with a diamond scribe. The sample diameter at the position of the tomographic section was generally smaller than 0.5 mm, the largest size of tungsten carbide/cobalt samples that could be imaged at a bending magnet source. Larger speci-

mens would require such a high x-ray energy that the x-ray flux at a bending magnet would be too small for efficient imaging (Fig. 2).

2.3 *Data Presentation*

The result of x-ray absorption tomography is two-dimensional maps of the x-ray absorption properties (the linear attenuation coefficient) in planes through the specimen, called tomograms. The linear attenuation coefficient expresses the probability per unit length for a photon to undergo an x-ray interaction process. The data constituting the tomograms can be presented in several ways. First, gray-scale images can be displayed, as shown in Fig. 3 and 4. The vertical color bar to the left in these images relates the reconstructed linear attenuation coefficient to the color in the image. In this case, dark colors represent low values of μ, light colors high values of μ. The minimum and maximum display values, in units of m^{-1}, are shown with the color bars. All values below and above these limits are displayed as black and white, respectively. By changing the display limits, the contrast in the displayed image can be enhanced, thereby visualizing all the information down to the limits of random noise. This presentation allows qualitative evaluation of the uniformity of the coatings and visualization of the void structures.

A complementary way of analyzing the data in the tomograms is to compute the frequency distribution of the pixel values. Plotting of these frequency functions, or histograms, may aid in obtaining an average for the reconstructed linear attenuation coefficient and gives a further indication of the homogeneity of the coating. When computing the histograms, it is important to exclude pixel values at the outer border of the sample, because these are subject to partial volume effects and have nothing to do with sample inhomogeneities. Figures 5 and 6 show the histograms obtained for the two tungsten carbide/cobalt specimens, and a summary of the experimental data is presented in Table 2.

Examination of the histograms in Fig. 5 and 6 shows that the peaks are approximately Gaussian with a full-width-at-half-maximum (FWHM) of 10 to 20% of the peak value. This spread results from noise, variations in specimen composition, density, and void structure. Again, it should be noted that void spaces smaller than the volume resolution of the CMT device, as well as the pixel values on the periphery of larger voids, are intermediate between those for air and a homogeneous coating. Therefore, they show up as a tail in the histograms.

In a two-phase system, it is possible to estimate the relative concentration of the two components from the measured linear attenuation coefficients and theoretical values of the two sample materials. Such analysis has not been attempted in the present study, because the x-ray energy spectrum obtained with the hafnium filter was fairly broad. By use of a monochromator, a narrow energy spectrum can be obtained and, thereby, more accurate values of the linear attenuation coefficients. Furthermore, using a subtraction image generated from two images obtained with energies above and below the K-absorption edge of tungsten, it would be possible to map the tungsten concentration through the specimens. This, however, would require a synchrotron source with higher energies than from a NSLS bending magnet, e.g., the X17 superconducting wiggler beam line of the NSLS.

Table 2 Analysis of plasma-sprayed WC/Co coatings using synchrotron-computed microtomography

Specimen No.	Pixel size, μm	Peak-average value linear attenuation coefficient, m^{-1}	Full-width-at-half-maximum of peak, m^{-1}
A98	3	4700	800
B99	4	6100	850

Note: A 254-μm hafnium filter was used on both specimens.

3. Discussion and Conclusions

The traditional problem associated with the characterization of imperfections in thermal spray deposits is to identify true pores from those created from polishing procedures. It is also very difficult to separate through-porosity from enclosed pores. Although the former pores can be characterized by methods of intrusion porosimetry, porosity caused by enclosed pores is not readily characterized. These limitations of metallographic analysis have been discussed widely.[3]

Although considerable progress has been made in quantitative image analysis, metallography still requires that the specimen preparation does not introduce voids, which might easily lead to subjective judgments. These CMT methods invite new opportunities for understanding the hitherto largely inaccessible imperfections in thermal spray coatings.

The externally injected plasma used to produce specimen A98 is supposed to produce a fairly porous deposit, whereas the internally injected plasma is supposed to produce a more homogeneous, or "dense" deposit specimen (B99). This was easily confirmed experimentally by examining the tomograms in Fig. 3 and 4. It is also clearly illustrated in the corresponding histograms shown in Fig. 5 and 6. The average value for the reconstructed linear attenuation coefficient for the A98 specimen is approximately 4700, and for the B99 specimen 6100. Note also in Fig. 5 that the distribution of reconstructed linear attenuation coefficients is asymmetric because of a tail on the low value side. This indicates a more inhomogeneous deposit.

Because the specimens imaged in this study were removed with a diamond scribe, it is possible that a fraction of the observed voids is due to cracking during the removal of the specimen from the support. Such cracking will also affect the shape of the histograms, which is indistinguishable from effects of other voids. It should be noted that the "optimum" sprayed coatings are the most difficult to remove, perhaps making them more vulnerable to damage during the removal process than more "poorly" sprayed coatings. In future work, a reproducible specimen preparation protocol will be introduced.

This first examination of thermal spray coatings using synchrotron CMT has successfully demonstrated its efficacy for examination of density variations and voids in these materials. The microscopic information that can be obtained is unique, because no specimen sectioning or polishing is necessary.

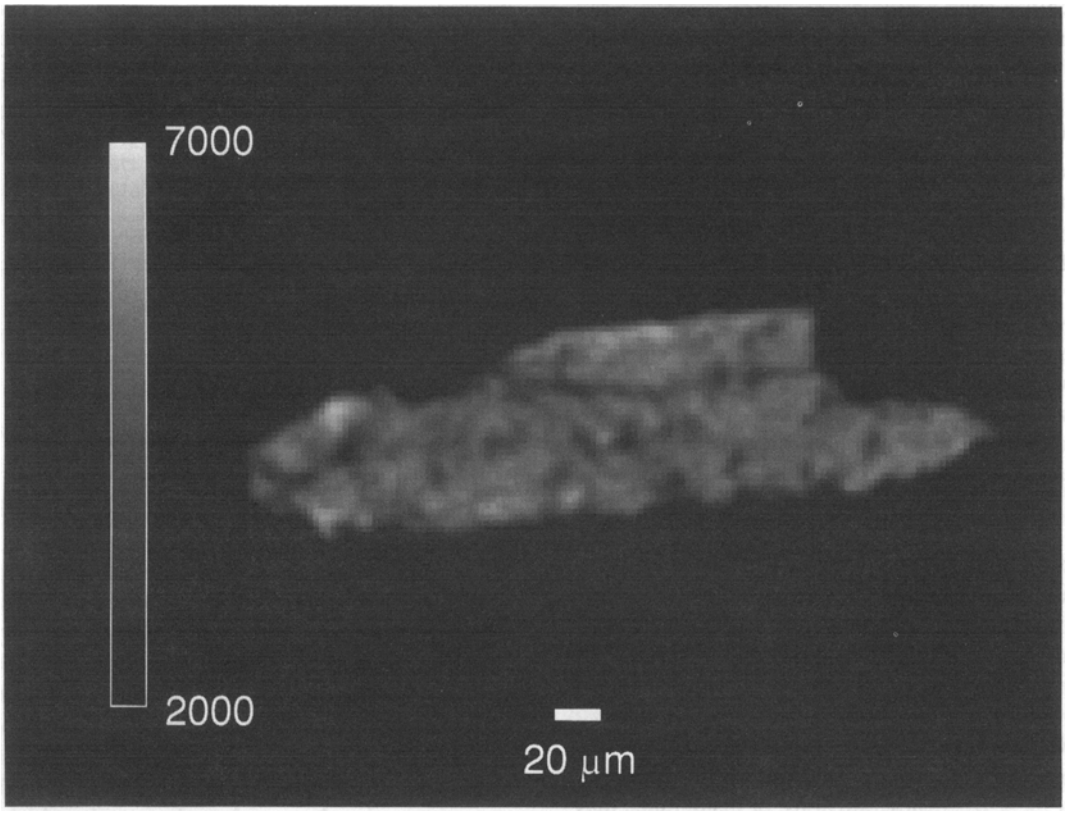

Fig. 3 Tomographic section of specimen A98 produced by an externally injected plasma.

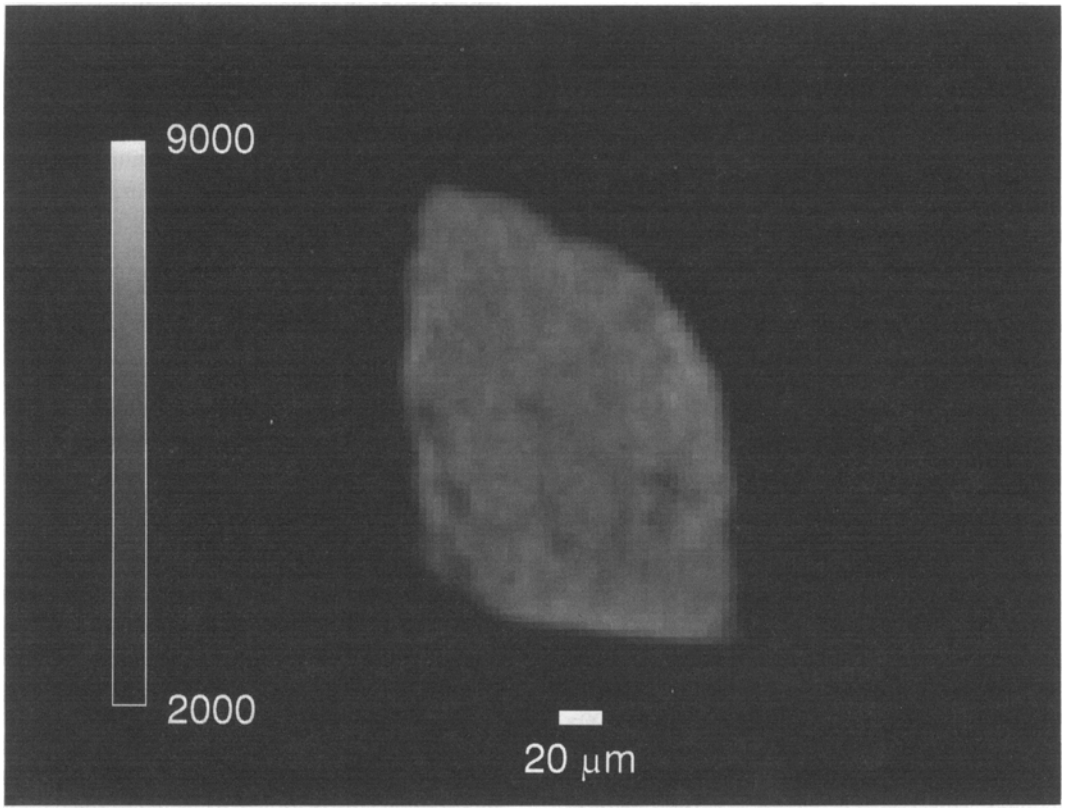

Fig. 4 Tomographic section of specimen B99 produced by an internally injected plasma.